Journal of Peptide Science
J. Peptide Sci. **5**: 442–456 (1999)

High Level of Aspartic Acid-bond Isomerization During the Synthesis of an *N*-Linked τ Glycopeptide

RALF HOFFMANN[a,b], DAVID J. CRAIK[c], KRISZTINA BOKONYI[a], ISTVAN VARGA[a] and LASZLO OTVOS JR[a,*]

[a] The Wistar Institute, 3601 Spruce Street, Philadelphia, PA, USA
[b] Biologisch-Medizinisches Forschungszentrum, Heinrich-Heine-Universität, Düsseldorf, Germany
[c] Centre for Drug Design and Development, University of Queensland, Brisbane, Australia

Received 20 April 1999
Accepted 13 May 1999

Abstract: An increased degree of utilization of the potential *N*-glycosylation site in the fourth repeat unit of the human τ protein may be involved in the inability of τ to bind to the corresponding tubulin sequence(s) and in the subsequent development of the paired helical filaments of Alzheimer's disease. To model these processes, we synthesized the octadecapeptide spanning this region without sugar, and with the addition of an *N*-acetyl-glucosamine moiety. The carbohydrate-protected, glycosylated asparagine was incorporated as a building block during conventional Fmoc-solid phase peptide synthesis. While the crude non-glycosylated analog was obtained as a single peptide, two peptides with the identical, expected masses, in approximately equal amounts, were detected after the cleavage of the peracetylated glycopeptide. Surprisingly, the two glycopeptides switched positions on the reversed-phase high performance liquid chromatogram after removal of the sugar-protecting acetyl groups. Nuclear magnetic resonance spectroscopy and peptide sequencing identified the more hydrophobic deprotected peak as the target peptide, and the more hydrophilic deprotected peak as a peptide analog in which the aspartic acid-bond just preceding the glycosylated asparagine residue was isomerized resulting in the formation of a β-peptide. The anomalous chromatographic behavior of the acetylated β-isomer could be explained on the basis of the generation of an extended hydrophobic surface which is not present in any of the other three glycopeptide variants. Repetition of the syntheses, with altered conditions and reagents, revealed reproducibly high levels of aspartic acid-bond isomerization of the glycopeptide as well as lack of isomerization for the non-glycosylated parent analog. If similar increased aspartic acid-bond isomerization occurs *in vivo*, a protein modification well known to take place for both the amyloid deposits and the neurofibrillary tangles in Alzheimer's disease, this process may explain the aggregation of glycosylated τ into the paired helical filaments in the affected brains. Copyright © 1999 European Peptide Society and John Wiley & Sons, Ltd.

Keywords: chromatography; Edman-degradation; nuclear magnetic resonance spectroscopy; paired helical filaments; β-peptide

Abbreviations: DIC, diisopropyl carbodiimide; DIEA, *N*,*N*-diisopropyl ethylamine; DMF, *N*,*N*′-dimethyl-formamide; DSS, 2,2-dimethyl-2-silapentane-5-sulfonate; ESI-MS, electrospray ionization mass spectrometry; Fmoc, 9-fluorenyl-methoxycarbonyl; GlcNAc, *N*-acetyl-glucosamine; HATU, 1-hydroxy-7-azabenzotriazole uronium salt; MALDI-MS, matrix-assisted laser desorption/ionization mass spectrometry; NFT, neurofibrillary tangles; NMR, nuclear magnetic resonance; NOE, nuclear Overhauser enhancement; NOESY, NOE spectroscopy; PHF, paired helical filaments; RP-HPLC, reversed-phase high performance liquid chromatography; TFA, trifluoroacetic acid; TBTU, 2-(1H-benzotriazole-1-yl)-1,1,3,3-tetramethyluronium tetrafluoroborate; TOCSY, total correlated spectroscopy.

* Correspondence to: The Wistar Institute, 3601 Spruce Street, Philadelphia, PA 19104, USA. E-mail: otvos@wistar.upenn.edu

CCC 1075–2617/99/100442-15$17.50

INTRODUCTION

One of the most dynamically developing areas of peptide chemistry is the synthesis of post-translationally modified peptides, most notably glycopeptides and phosphopeptides [1–3]. These modified peptides are used for studying the role of sugar or phosphate incorporation on the recognitional [4,5], conformational [6], stability [7], or other properties of fragments of glyco- or phosphoproteins. The post-translationally modified peptides are also attractive alternatives to existing peptide modification methods in biotechnology [8,9]. Owing to the relatively mild reaction conditions, Fmoc-solid-phase synthesis is the method of choice for the preparation of glycopeptides and phosphopeptides. These syntheses are significantly facilitated by the commercial availability of mono- and disaccharide-containing, sugar-protected, Fmoc-Asn/Ser/Thr derivatives, or phosphate-protected Fmoc-Ser/Thr/Tyr derivatives. Most of the available troubleshooting efforts focused on the development and application of the building blocks themselves [10,11], understandably so as the assembly of complex carbohydrate systems and sugar–peptide connections require highly sophisticated chemistry [12]. However, due to the relative lack of in-depth synthetic experience with the commercially available protected (and sometimes activated) glycoamino acids, peptide sequence-specific side-reactions have not been, or have very rarely been reported during custom solid-phase synthesis of glycopeptides.

Approximately 10 years ago we showed that Fmoc-Asn(GlcNAc)-OH, with free sugar hydroxyl groups is superior to Fmoc-Asn(Ac_3GlcNAc)-OH for solid-phase glycopeptide synthesis because of the lack of acetyl transfer during the synthesis and deprotection steps [13]. Notwithstanding the validity of this statement, the variable yields of the preparation of Fmoc-Asn(GlcNAc)-OH or of the unprotected disaccharide derivative Fmoc-Asn-(chitobiose)-OH [14] and the slow but measurable decomposition of these reagents during storage makes Fmoc-Asn(Ac_3GlcNAc)-OH the commercially preferred *N*-glycopeptide building block. We used this acetylated reagent in the preparation of a glycosylated version of the fourth repeat unit of human τ protein (τR4-G), and in the current report we detail unexpected synthetic and chromatographic peptide behavior we encountered during glycopeptide preparation and analysis. In particular, we found substantial β-aspartate formation, an event undetectable during the synthesis of the parent, non-glycosylated analog (τR4), and a delay of the elution of the peracetylated, isomerized glycopeptide during reversed-phase high performance liquid chromatography (RP-HPLC) (Table 1).

The synthetic τR4 and τR4-G peptides are potentially useful reagents to study the development of the neurofibrillary tangles (NFT) of Alzheimer's disease. The NFT, one of the proteinaceous aggregates found in the brains of the affected patients, are formed from the low molecular weight microtubule-associated protein τ [15]. τ proteins, isolated from NFT, are organized as paired helical filaments (PHF-τ) [16]. PHF-τ is abnormally hyperphosphorylated on nearby serine and threonine residues [5,17] but it is still not established whether excessive phosphorylation is the reason for τ assembly in PHF, or phosphorylation is a consequence of an unrelated aggregation process [18]. Recently Iqbal and colleagues documented that PHF-τ is *N*-glycosylated while normal τ is not [19]. Careful examination of the τ sequence reveals only two potential *N*-glycosylation sites, Asn359 and Asn410. Asn359 is located in the fourth repeat unit of τ. Since normal τ binds to tubulin through the 18-mer repeat domains [20], it is reasonable to hypothesize that glycosylation of the Asn in the fourth repeat will interfere with microtubule assembly. Indeed, at the synthetic peptide level, incorporation of GlcNAc prevents τR4 from binding to the highly acidic *C*-terminal τ-binding dodecapeptide of β-tubulin [21]. Although these observations can explain the lack of functional τ in the affected brains, they can not explain how deranged τ can be involved in the deposition process. Based on our synthetic observations, we are now able to provide such an explanation. Clearly the reaction conditions are completely different during peptide synthesis or *in vivo* protein transformation. Nevertheless, the thermodynamics of these reactions can favor identical final products. Accordingly, if abnormally excessive glycosylation of Asn359 was the first event in τ derangement and an aspartic acid-bond isomerization, a process is known to produce protease-resistant protein variants followed this event *in vivo*, this cascade may be able to lead to the accumulation of τ into the PHFs.

MATERIALS AND METHODS

Peptide Synthesis

Peptides were synthesized according to standard solid-phase protocols using Fmoc-*N*-terminal

protecting strategy [22]. Non-glycosylated peptide τR4 and its glycosylated analog, τR4-G, were made using an identical protocol to obtain a comparison between the crude products of the two syntheses. For this purpose, the peptides were assembled on a Rainin PS 3 automated synthesizer on Tentagel S RAM resin (Rapp Polymere, Tubingen, Germany). Amino acids were activated with 2-(1H-benzotriazole-1-yl)-1,1,3,3-tetramethyluronium tetrafluoroborate (TBTU), 1-hydroxy benzotriazole (HOBt), and *N*,*N*-diisopropyl-ethylamine (DIEA), and were added in a four molar excess to the amino-resin in *N*,*N*′-dimethyl-formamide (DMF). The coupling time was 30 min. The glycoamino acid was incorporated as Fmoc-Asn(Ac_3GlcNAc)-OH (purchased from Bachem, King of Prussia, PA). To save reagent, the glycoamino acid was coupled only with a 10% excess. The resin was removed from the reaction vessel, and an equimolar mixture of Fmoc-Asn(Ac_3GlcNAc)-OH, diisopropyl carbodiimide (DIC), and DIEA, dissolved in DMF:*N*-methyl-pyrrolidone (1:1; v/v), was added. After 6 h, fresh DIC was added and the reaction was allowed to proceed overnight. After the coupling step of the glycoamino acid, the ninhydrin test of the resin [23] was negative. Upon removal of the Fmoc-group and a test cleavage, the protected glycopeptide showed a single peak on RP-HPLC. The resin was placed back to the synthesizer, and the rest of the peptide assembly was continued automatically. Repetitive *N*-terminal deprotection was achieved with 20% piperidine dissolved in DMF in two steps, for 5 min each. After the chain assembly was completed, the peptides were cleaved off the solid support with a mixture of 5% thioanisole, 5% water, 5% *m*-cresol and 2.5% ethanedithiol in trifluoroacetic acid (TFA) at room temperature for 2 h. The carbohydrate protecting acetyl groups were removed by a 15 min treatment with 0.02 M NaOH [24]. Table 1 lists the peptides, the RP-HPLC retention times and the matrix-assisted laser desorption/ionization mass spectrometry (MALDI-MS) data used for characterization of this first set of products.

The syntheses were repeated by using different conditions to verify the lack of aspartic-acid bond isomerization for the non-glycosylated peptide and the presence of the β-peptide formation of the glycopeptide, regardless of the methods used for their preparation. For this purpose, τR4 was assembled on an Applied Biosystems 433A batch synthesizer

Table 1 Synthetic Peptides of this Study and Some of the Analytical Data from the First Set of Syntheses

Peptide[a]	Sequence[b,c]	Retention time of RP-HPLC (min)	MALDI-MS $[M+H]^+$ (Da)
τR4 (amino acids 350–367)	VQSKIGSLDNITHVPGGG	25.8	1779.4
τR4 Ac_3 GlcNAc peak 1	VQSKIGSLDN(Ac_3-β-GlcNAc)ITHVPGGG COOH	27.9	n.d.[d]
τR4 Ac_3 GlcNAc peak 2	VQSKIGSLD-COOH N(Ac_3-β-GlcNAc)ITHVPGGG	28.6	n.d.
τR4 GlcNAc 1706	VQSKIGSLDN(β-GlcNAc)ITHVPGGG COOH	25.0	1981.8
τR4 GlcNAc 1709	VQSKIGSLD-COOH N(β-GlcNAc)ITHVPGGG	23.7	1982.2

[a] The names of the peptides correspond to the RP-HPLC fraction numbers (peracetylated glycopeptides) or to the appropriate chromatogram numbers (deacetylated glycopeptides).
[b] The identity of the glycopeptides was determined by ESI-MS/MS, peptide sequencing and NMR (see 'Results'). The free carboxyl group of Asp9 is emphasized to distinguish the 'normal' and isomerized glycopeptides.
[c] The peptides had free amino termini and were *C*-terminal amides.
[d] Mass spectra of the acetylated peptides (intermediate products) were not collected at the time of the first synthesis.

using FastMoc chemistry in a 0.1 mmole scale. The amino acids were added in a 10 M excess. The synthesis of the glycopeptide was repeated on the Rainin PS 3 synthesizer, but this time the activating reagent was 1-hydroxy-7-azabenzotriazole uronium salt (HATU), and the glycoamino acid was coupled during a regular cycle in a 4 M excess. As with the second synthesis of the non-glycosylated peptide, very fast cycles were used. The time required for coupling, washing, deprotection and repeated washing steps remained below 1 h. The glycopeptide was cleaved from the resin with a 2 h treatment with 5% thioanisole and 1% water in TFA. Other parameters for peptide synthesis remained unchanged.

Chromatography

The HPLC system consisted of two Beckman 110B solvent delivery modules and a Beckman system organizer, driven by a NEC PC 8300 controller. A Rainin Dynamax absorbance detector model UV-C was set to 214 nm, and the chromatograms were recorded on a Shimadzu CR501 Chromatopac integrator. A Phenomenex Jupiter C18 silica column (5 μm particle size and 300 Å pore size) was used. Solvent A was 0.1% aqueous TFA, solvent B was acetonitrile containing 0.1% TFA. A gradient of 1.33% solvent B/min was applied at a flow rate of 1 ml/min starting from 5% B solvent composition. The integrity of the purified peptides was verified by MALDI-MS. Mass spectra were recorded at the Wistar Institute Protein Microchemistry Facility on a Voyager Biospectrometry Workstation.

Electrospray Ionization (ESI) MS and ESI-MS/MS

ESI spectrometry was performed using a VG Biotech BIO-Q instrument with quadrupole analyser at M-Scan, Inc. (West Chester, PA). Myoglobin was used to calibrate the instrument, and elution was carried out with 50% aqueous acetonitrile containing 0.1% TFA. ESI-MS/MS was performed using a Quattro II upgraded BioQ triple quadrupole instrument. Daughter ion spectra were generated from the appropriate doubly-charged parent ion at m/z 991 using argon as a collision gas. Collision energy and gas cell pressure were varied in order to optimize the MS/MS spectrum.

Peptide Sequencing by Edman-degradation

Peptides were sequenced on a 476A protein sequencer (PE Biosystems, Weiterstadt) using the Microcartridge and the standard chemistry supplied with the instrument. Fifty to 200 pmoles of the purified peptides was added to a BioBrene Plus (PE Biosystems) coated membrane and sequenced in the pulsed-liquid mode.

Molecular Modeling

Probable three-dimensional structures were generated using simulated annealing and energy minimization protocols with the Quanta software package (version 4.1.1). A simulated annealing protocol was used to generate a set of 180 structures starting from template structures built up according to secondary structure prediction [25]. The assignment of the amino acids were as follows: Val1-Gln2-β-sheet; Ser3-Asn10-type I β-turn, Ile11-Val14-β-sheet; Pro15-Gly18-type II β-turn. Circular dichroism spectroscopy in trifluoroethanol–water mixtures verified the predominantly type I β-turn character of the non-glycosylated peptide. The calculation protocol consisted of a total of 4.5 ps molecular dynamics (900 K), including warm-up. For each peptide, four low energy conformers were selected randomly from different regions of the trajectory of the high temperature simulation. The structures were cooled down to 300 K over 2.7 ps, and were subjected to 2000 cycles of energy minimization by using the steepest descent algorithm under the influence of the CHARMm force field [26]. Parameter and topology files for the preassembled GlcNAc moiety were taken from the Quanta library files, included in the software package.

Nuclear Magnetic Resonance (NMR) Spectroscopy

^{1}H-NMR spectra were recorded on a Bruker DMX 750 MHz spectrometer at 298 K for solutions of the peptides (< 1 mM) in 90% H_2O/10% D_2O. Two-dimensional NMR spectra were recorded in the phase sensitive mode using time proportional phase incrementation for quadrature detection in the f1-dimension [27]. Solvent suppression for NOESY and TOCSY experiments was achieved using the WATERGATE pulse sequence while preirradiation of the water signal was used in 1D spectra. Chemical shifts were referenced to DSS. The TOCSY spectra were recorded using an MLEV-17 mixing scheme [28] with a mixing time of 80 ms. The mixing time in the NOESY spectrum was 350 ms. Two-dimensional spectra were collected over 4096 data points in the f2 dimension, generally with 512 increments in f1, each of 32–128 scans. The spectra were acquired

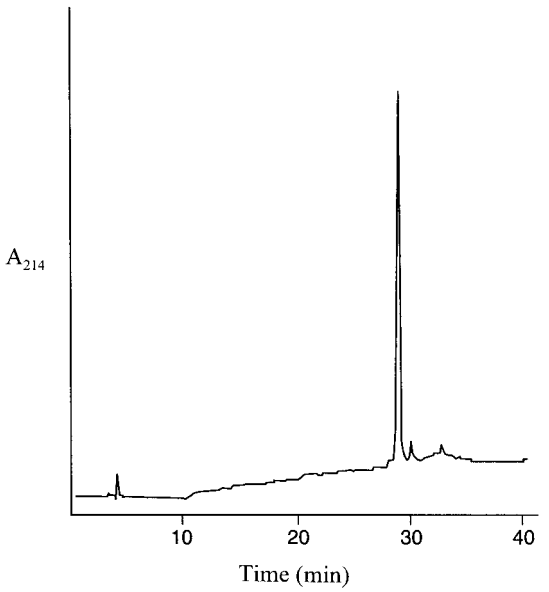

Figure 1 RP-HPLC trace of the crude product after the synthesis of unmodified peptide τR4. A single peak was observed. This HPLC profile represents the repeat synthesis; the delay of the elution time compared to that in Table 1 reflects the aging of the column.

over a spectral width of 12 ppm in both dimensions. The data were processed on a Silicon Graphics (SGI 4D/30) computer using the UXNMR software package. The f1-dimension was zero-filled to 4096 real data points, with f1- and f2-dimensions being multiplied by a squared sine function and Gaussian function, respectively, prior to Fourier transformation. Polynomial baseline correction was used in f2.

RESULTS

Analysis of the Synthetic Crude Products

The solid-phase synthesis of unmodified peptide τR4 proceeded without difficulty. The RP-HPLC profile of the crude product revealed a single peak (Figure 1). MALDI-MS, peptide sequencing and NMR identified the purified peptide as the target molecule. No major reduction of the amino acid recovery following Leu8 was observed during the solid-phase sequencing confirming that the peptide consisted of only α-amino acid residues (Figure 2).

During the first synthesis of the glycopeptide we checked the integrity of the resin-bound τR4 fragment before the glycoamino acid was added. When a test cleavage of the Ile11-Gly18 resin was made, the peptide showed a single peak on HPLC eluting at 18.6 min (data not shown). The peptide assembly was completed by addition of the Fmoc-Asn(Ac_3GlcNAc)-OH residue followed by residues Asp9-Val1. After cleavage, the crude product showed two HPLC peaks, in approximately equal ultraviolet intensities (Figure 3). The two peaks were separated, and the products deacetylated by a short treatment with 0.02 M NaOH. We have previously shown that a controlled use of diluted NaOH has no deleterious effects on peptide composition and purity when used for the removal of sugar-protecting acetyl groups [29]. In spite of the large number of aspartic acid-containing glycopeptides that were deacetylated with 0.01–0.1 M NaOH, no aspartimide formation had previously been observed [7,30,31]. Similar to these earlier observations, the purified τR4 Ac_3GlcNAc HPLC fractions remained essentially single peaks after 0.02 M NaOH treatment; with the deacetylated glycopeptides eluting earlier than the acetylated counterparts, as expected (Figure 4). Finally, the acetyl-free glycopeptide fractions were subjected to another round of RP-HPLC purification. The purified glycopeptides remained single peaks after repeated treatments with 100% TFA or 0.01 M aqueous NaOH.

It was interesting to note that the order of the HPLC retention times was reversed after removal of the sugar-protecting acetyl groups. The retention time of τR4 Ac_3GlcNAc peak 1 (27.9 min) decreased by 2.9 min (to 25.0 min) and the retention time of τR4 Ac_3GlcNAc peak 2 (28.6 min) decreased by 4.9 min to 23.7 min (Table 1). We recently prepared three additional, unrelated *N*-glycopeptides with identical synthetic and chromatographic strategies. These glycopeptides carried the Asn(GlcNAc) residue in either *N*-terminal, mid-chain, or *C*-terminal positions. The retention times after removal of the sugar-protecting acetyl groups decreased by 2.8, 2.6 and 2.2 min, respectively. Based on this analogy, the 2.9 min decrease of the retention time for τR4 Ac_3GlcNAc peak 1 fell in line with expectations. The 4.9 min value for τR4 Ac_3GlcNAc peak 2, however, seemed unusually high. Apparently secondary structure formation caused the delayed RP-HPLC elution of τR4 Ac_3GlcNAc peak 2 (or, alternatively, accelerated the elution of its deacetylated counterpart, τR4 GlcNAc 1709).

The two final glycopeptides, τR4 GlcNAc 1709 (earlier eluting compound) and τR4 GlcNAc 1706 (later eluting compound) were submitted for mass spectrometry to shed light onto the compositional difference between the two products. First, MALDI-MS was performed but no difference in the mass

spectra was detected (Table 1). The observed 1982 Da for both τR4 GlcNAc 1709 and τR4 GlcNAc 1706 corresponded to the expected molecular mass of the target glycopeptide. For more accurate results, the glycopeptides were analysed by ESI-MS and ESI-MS/MS. In the direct electrospray spectra, both glycopeptides appeared to have the same probable $[M+H]^+$ pseudomolecular ion with a mass of 1980.3 (monoisotopic) and both samples showed a similar pattern of fragmentation. The two ESI-MS/MS spectra were extremely similar showing a number of major possible daughter ion fragments which were assigned to the anticipated sequence (Figures 5 and 6). A number of additional signals were also observed and these probably arose from alternative fragmentation mechanisms. However, these ions were detected in both samples. The mass spectrometry data showed that the only potential differences between the two glycopeptides could be positional or geometric isomerism, for example, aspartate-bond isomerization at Asp9, or *cis*/*trans* isomerization at Pro15.

Identification of β-aspartate by ^{1}H-NMR Spectroscopy

A series of 1D and 2D NMR spectra of glycopeptides τR4 GlcNAc 1706 and τR4 GlcNAc 1709 and the non-glycosylated peptide was recorded to determine the origin of their different chromatographical properties. For the non-glycosylated peptide 1D, TOCSY and NOESY spectra were recorded and a full sequential assignment of all spectral peaks was achieved. For the two glycosylated peptides sufficient material was available only for 1D and TOCSY spectra, and sequential assignments were made by analogy with those in the non-glycosylated peptide. It is clear from an analysis of the NMR spectra that the sugar residues are identical in both glycosylated peptides. This is based on the observation of TOCSY cross peaks in both glycopeptides (but not in the non-glycosylated peptide) which clearly show connectivity between an anomeric proton at approximately 5.05 ppm and other sugar protons in the chemical shift range 3.40–3.90 ppm. The shift of the anomeric proton in both glycopeptides is highly

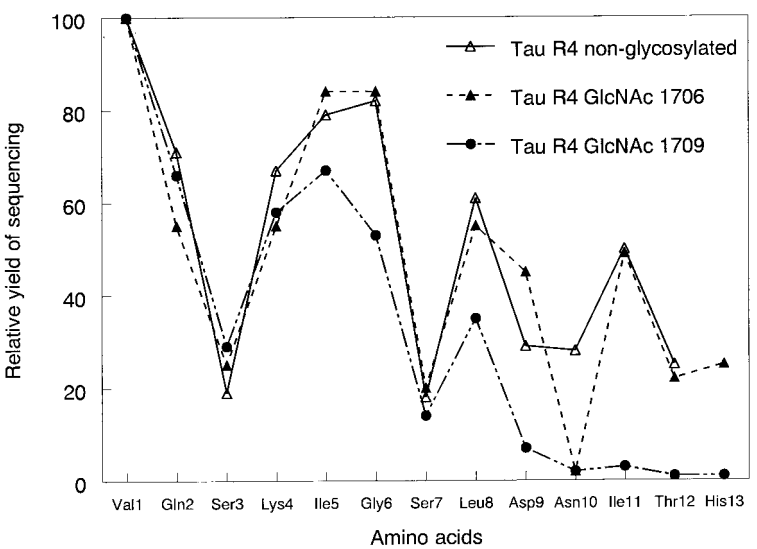

Figure 2 Solid-phase sequencing of peptides τR4, and the two glycopeptide analogs. Solid line and open triangles represent the non-glycosylated peptide. The 'normal' glycopeptide is represented by broken lines and full triangles, and the isomerized glycopeptide is represented by dots and dashes and full circles. The amino acid recovery did not significantly decrease for the unmodified peptide and for the later eluting glycopeptide product [except at the two serines for which the recovery is always below the other amino acid residues and at Asn(GlcNAc)10 which cannot be detected with the methodology used], but the sequencing stalled at Asp9 of the earlier eluting glycopeptide. It is best to compare the yields of Ile5 (before the isomerized Asp9) and Ile11 (after the glycoamino acid Asn10). The repetitive yields are just below 95% (the accepted level) for the non-glycosylated peptide and the 'normal' glycopeptide, and below 5% of the isomerized glycopeptide. The products of the repeat syntheses were used for these analyses.

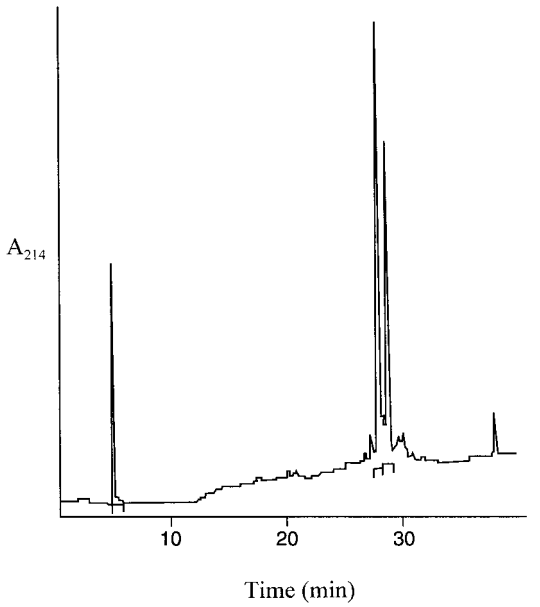

Figure 3 RP-HPLC trace of the crude product after the synthesis of carbohydrate-protected glycopeptide τR4 Ac_3GlcNAc. The two peaks were separated, labeled as Ac_3GlcNAc peak 1 (earlier eluting peptide) and Ac_3GlcNAc peak 2 (later eluting peptide). Ensuing deacetylation and analysis of the final products identified peak 1 as a glycopeptide containing α-peptide bond and peak 2 as containing a β-peptide bond between Asp9 and Asn10.

characteristic of β-linked GlcNAc, as is a peak for H-4, which is well resolved at 3.45 ppm in the 1D spectrum shown in Figure 7. This peak, as expected, is absent from the non-glycosylated peptide. The identity of H-1 and H-4 signals in both glycosylated peptides and their similarity with literature shifts for β-GlcNAc unequivocally confirms that the sugar parts of both glycopeptides are identical and that no unusual anomerization, substitution or rearrangement of the sugar residue has occurred in either of the glycopeptides. The observed chromatographical differences between the two glycopeptides was therefore concluded to involve the peptide backbone.

Turning to the peptide backbone, the Hα chemical shifts for the non-glycosylated peptide are not significantly different (i.e. within 0.1 ppm) from random coil values, suggesting that the peptide does not have a well defined conformation in solution as is common for linear peptides of this size. There are some minor changes in chemical shifts of the glycosylated peptides relative to the parent peptide, suggesting that glycosylation does induce small changes in the relative populations of individual conformers amongst the conformational ensemble. This is illustrated by the differences in the methyl region of the 1D spectrum shown in Figure 8, a region that is generally sensitive to the global fold of peptides and proteins. The later eluting glycopeptide τR4 GlcNAc 1706 appears to be more similar to the non-glycosylated peptide than is the earlier eluting glycopeptide τR4 GlcNAc 1709, and the two glycopeptides are clearly different from each other, supporting the interpretation from HPLC that the molecules are different species. Of the various possible explanations for the differences between the peptides the differences appear not to be due to *cis*/*trans* isomerization about the Val-Pro bond. NOESY data for the non-glycosylated peptide shows that this bond adopts the *trans* conformation. The chemical shifts of the Pro resonances are similar in all three peptides and, by analogy, all likely adopt the *trans* conformation. It is more likely that the differences between the two glycosylated forms reflect isomerization of the aspartic acid residue adjacent to the glycosylation site. Analysis of TOCSY

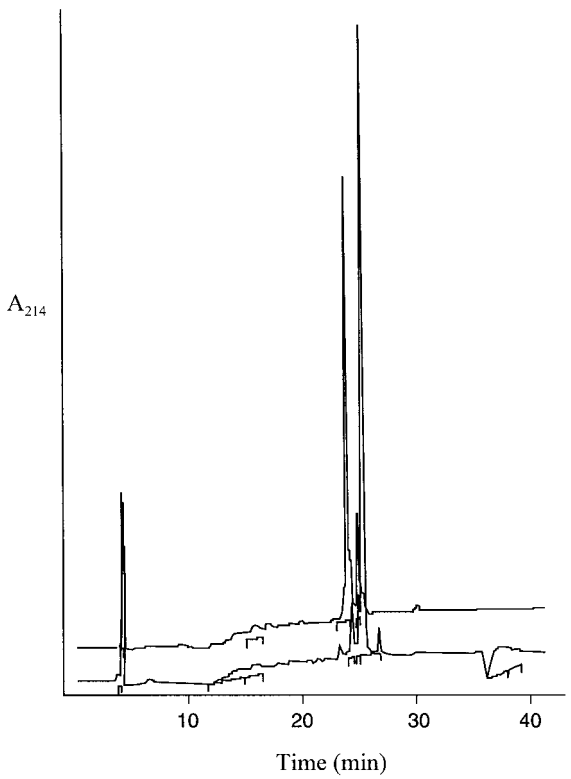

Figure 4 A composite chromatogram of the crude products after deacetylation of τR4 Ac_3GlcNAc peak 1 (lower trace) and τR4 Ac_3GlcNAc peak 2 (upper trace). The elution order is reversed after removal of the sugar-protecting acetyl groups.

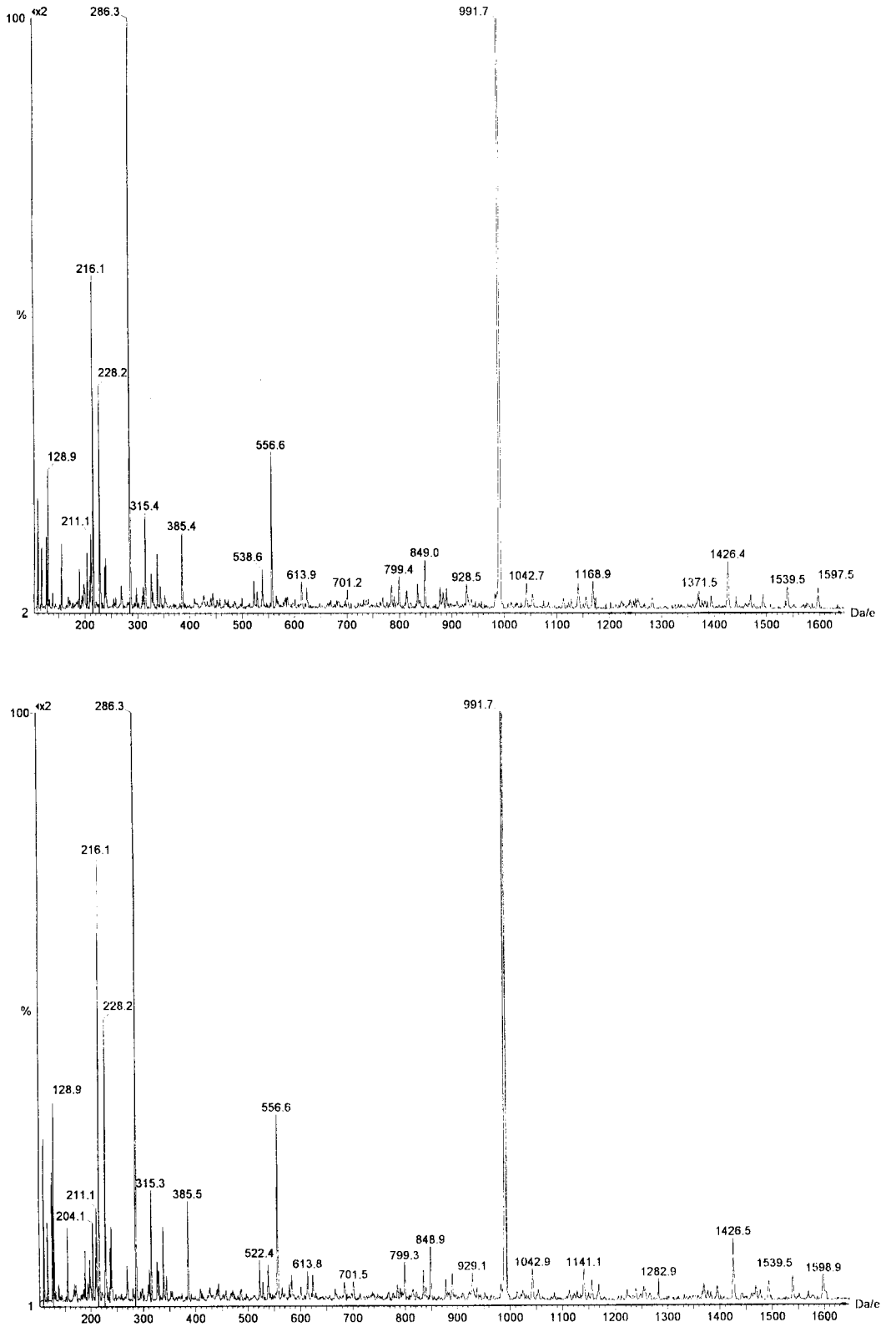

Figure 5 ESI tandem mass spectra of glycopeptides τR4 GlcNAc 1706 (top) and τR4 GlcNAc 1709 (bottom). The spectra are extremely similar and show a number of identical possible daughter ions of the double-charged molecular ion at 991 *m*/*z*.

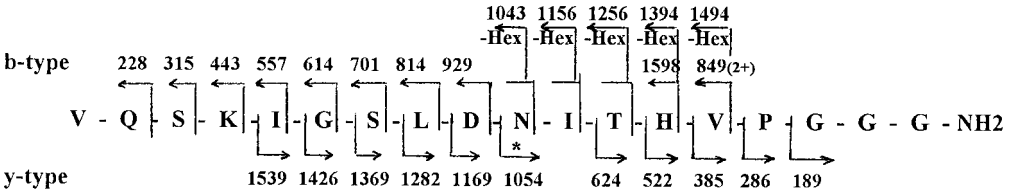

Figure 6 Daughter ions that can be assigned based on the fragmentation pattern from the electrospray-ionization tandem mass spectra. The star under Asn10 indicates the attachment site of the *N*-acetyl-glucosamine moiety (labeled as Hex). The peptide fragments identify the glycopeptides as the target τR4 GlcNAc sequence.

spectra shows that the chemical shifts for Hα of Asp9 in the parent peptide and in the later eluting and the earlier eluting glycopeptides are 4.54, 4.54 and 4.38 ppm, respectively. The significantly different Asp9 Hα shift is consistent with the presence of β- rather than α-aspartic acid in glycopeptide τR4 GlcNAc 1709, while the other two peptides contain the conventional α-aspartic acid. The similarity of Hα shifts for the parent peptide and glycopeptide τR4 GlcNAc 1706 implies a minimal effect of adjacent glycosylation on Asp9 when there is no isomerization. Indeed, the Hα shifts of the glycosylation site itself, Asn10, are similar in all three peptides (4.66, 4.68 and 4.65 ppm). Likewise, there are only minor differences in the Hβ shifts of Asp9 and Asn10 in the three peptides, as illustrated in Figure 7.

Isomerization to β-Asp would not be expected to cause a large change in chemical shift of the Hβ protons of Asp9, but the observed increase in separation of these diasterotopic protons in TOCSY spectra of the earlier eluting glycopeptide (0.14 ppm) compared with the later eluting glycopeptide (0.08 ppm) and the parent non-glycosylated peptide (0.09 ppm) is consistent with β-Asp formation in glycopeptide τR4 GlcNAc 1709. In the spectrum of glycopeptide τR4 GlcNAc 1706 shown in Figure 7 there is a second set of peaks associated with the Hβ protons of Asn10, having an intensity approximately one-third that of the main signals. This most likely reflects the presence of *cis*/*trans* isomerization about the amide bond in the glycosidic linkage between Asn10 and GlcNAc. This additional degree of conformational variability was not detected for the earlier eluting glycopeptide, however the poorer signal to noise in the spectra of this peptide may have precluded its detection if present.

Sequencing of the τR4 GlcNAc Glycopeptides

The two final glycopeptides were submitted to Edman-degradation and peptide sequencing to verify the aspartic acid-bond isomerization for the earlier eluting variant. In order to retain the peptides during the sequencing, they were adsorbed to the surface of BioBrene coated cellulose membranes. Strong ionic interactions between the peptides and the membrane warrant improved peptide recovery at even distant sequencing cycles. The Edman-degradation went smoothly until Asp9 of the later eluting τR4 glycopeptide. Because of glycosylation of Asn10, there was no Asn-signal detected in the tenth cycle, but the Ile was clearly identified in the eleventh cycle, as well as the consecutive amino acid residues Thr12 and His13 (Figure 2). This pattern of Edman-degradation of an *N*-glycopeptide was identical to that of our control glycopeptide (a pentadecapeptide corresponding to the first potential *N*-glycosylation site of the myelin oligodendrocyte glycoprotein) in which the lack of Asp residue excludes the formation of any β-peptide bond. In contrast, when the sequencing of the earlier eluting τR4 glycopeptide was attempted, the Edman-degradation stalled after Leu8, and no further amino acid could be identified (Figure 2). This finding indicates that the earlier eluting τR4 glycopeptide did not contain an α-peptide bond in position 9. We concluded that only isomerization of Asp10 could be responsible for the complete signal loss.

DISCUSSION

Aspartic acid-bond isomerization is considered a potentially frequent side-reaction during the preparation of peptides [32,33]. However, with the widespread utility of Fmoc-chemistry and the advent of fast coupling and deprotection cycles and reagents, the level of this side reaction is usually equivalent or below the level of other unwanted products during standard solid-phase peptide synthesis [34]. In spite of the large number of peptides that we have prepared on our Milligen 9050 and Rainin PS 3 synthesizers in the past 10 years, we have never

encountered significant amounts of aspartimide formation until the synthesis of the τR4 glycopeptide. This peptide sequence contains an Asp-Asn fragment, which is known to be prone to aspartimide formation during Fmoc-chemistry [35]. Nevertheless, when the crude product of the synthesis of the unmodified τR4 peptide was analysed, no aspartic acid-bond isomerization was detected.

Surveying all the *N*-glycopeptides we have made so far, only five contained aspartic acid residues within the sequence. We did not notice any aspartimide formation during the solid-phase assembly of these glycopeptides. Nevertheless, no aspartic acid is found *N*-terminal to the glycosylated Asn in these sequences. This fact may be related to our practice of modeling the glycoprotein fragments with the glycopeptides, coupled with the observation that the occurrence of Asp in -1 position to utilized or unutilized potential *N*-glycosylation sites of proteins is 3.8% and 2.1%, respectively [36], values well below the average of 5.3% Asp in 1465 unrelated sequences that are claimed to model the statistical distribution of amino acids in proteins well [37]. Four of the five Asp-containing glycopeptides we made earlier were synthesized by using Fmoc-Asn-(sugar)-OH derivatives with unprotected carbohydrate-hydroxyl groups [38]. In this regard, the τR4 GlcNAc glycopeptide can be considered unique both in amino acid sequence and mode of preparation. However, the recently introduced commercial availability of the Fmoc-Asn(Ac_3GlcNAc)-OH derivative and the well-deserved current popularity of glycopeptides suggests an increase in the number of synthetic glycopeptides containing the Asp-Asn dipeptide fragment and the use of the Fmoc-Asn(Ac_3GlcNAc)-OH monomer for their synthesis.

The non-glycosylated peptide could be made reproducibly without aspartic acid isomerization, whereas the glycopeptide was isomerized in both syntheses. Two different activation strategies were selected for both peptides to make sure that the first findings were not due to particular reaction conditions. The only difference between the DIC- and the HATU-mediated syntheses was the presence of partially deacetylated glycopeptides following the TFA cleavage when HATU was used. Nevertheless, the use of HATU is highly recommended for the coupling of sterically hindered amino acids [39] such as peracetylated Fmoc-glycoamino acids. The off-synthesizer activation of the Fmoc-protected glycoamino acid during the first reaction resulted in cleaner reaction products, but the completely automatic synthesis at the second attempt proceeded considerably faster. Practitioners are warned to define their individual preferences before synthesis.

We were looking for potential reasons for the aspartimide formation of the glycopeptide when such

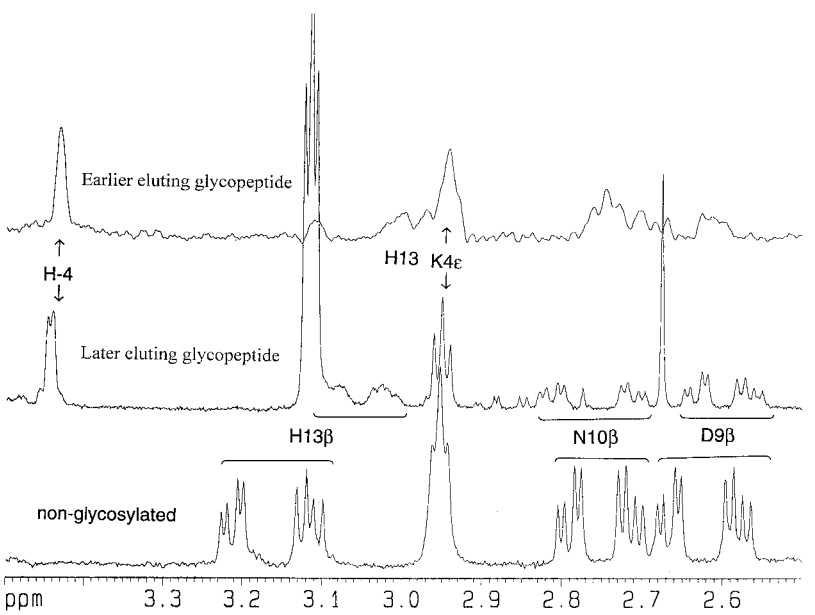

Figure 7 Region of the 750 MHz 1D NMR spectra of the non-glycosylated peptide τR4, glycopeptide τR4 GlcNAc 1706 and glycopeptide τR4 GlcNAc 1709, which includes peaks from the Hβ protons of Asp9 and Asn10. The peak marked H-4 is characteristic of β-linked GlcNAc.

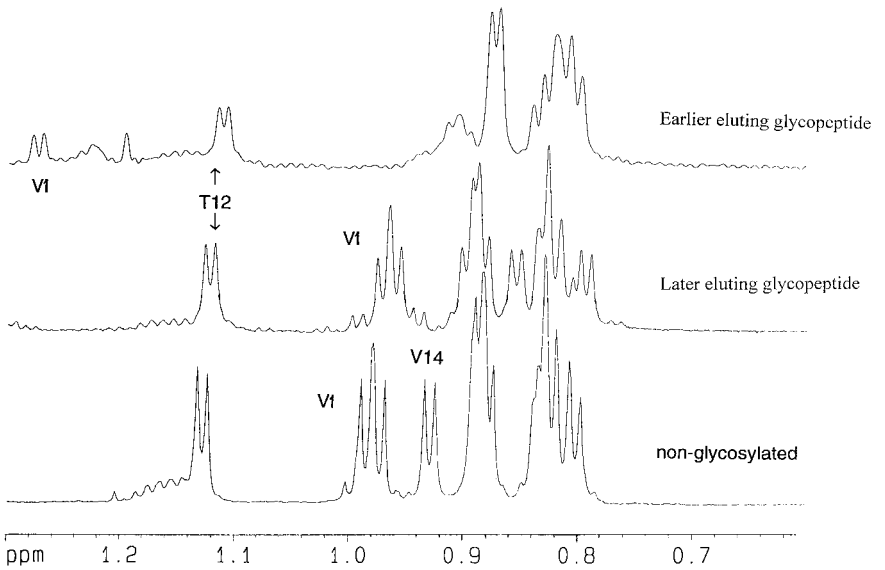

Figure 8 Methyl region of the 750 MHz 1D NMR spectra of the non-glycosylated peptide τR4, glycopeptide τR4 GlcNAc 1706 and glycopeptide τR4 GlcNAc 1709. Selected methyl peak assignments are indicated.

a modification was absent during the synthesis of the unmodified parent analog. At the present time no explanation can be formulated based on simple electric or steric phenomena. The Asn10 was protected with the trityl group during the preparation of the non-glycosylated peptide, and with the peracetylated carbohydrate during the synthesis of the glycopeptide. Both Asn protecting groups are bulky, and potentially minimize succinimide formation between Asn10 and Asp9 [33]. For a base-catalysed succinimide formation to take place, the proton from the amino nitrogen of the Asn10 has to be abstracted, and it is highly unlikely that the sugar moiety would have a strong through-space electron-donating effect to aid the amino proton removal when the trityl group lacks such an effect. Another possibility is a conformational difference leading to an increased tendency of the glycopeptide to form the succinimide derivative [35]. If the amino nitrogen of the Asn10 was closer to the carbon of the β-carboxyl group of the Asp9 in the glycopeptide than in the non-glycosylated variant, this would explain the differences in the rate of succinimide formation. To explore this scenario, we modeled the non-glycosylated and the 'normal' glycosylated peptides, still in the fully protected form, as they existed during the synthesis. The peptides were built up from segments of type I and type II β-turns and extended structures, based on secondary structural prediction and circular dichroism spectroscopy. A simulated annealing protocol was applied, and for each peptide four low energy conformers were randomly selected from various points of the high temperature trajectory. The four structures were nearly identical for both peptides verifying the validity of the initial structures and the annealing algorithm. The measured average distances between the β-carbon of the Asp9 and the amino nitrogen of the Asn10 were 4.3 Å for the non-glycosylated τR4 peptide and 4.7 Å for the glycopeptide (both contained only α-amino acids), excluding the possibility of simple steric reasons for the aspartimide formation of the glycosylated variant.

Changes in the NMR spectra of the three peptides are consistent with the presence of β-Asp in the earlier eluting glycopeptide, and α-Asp in the later eluting glycopeptide and the parent non-glycosylated analog. The major changes are an upfield shift of the Hα proton of Asp9 and an increased separation of its diastereotopic Hβ protons in glycopeptide τR4 GlcNAc 1709 relative to the other peptides. The latter change is consistent with a greater degree of conformational restriction of the β-methylene group when it is incorporated into the peptide backbone (in β-Asp) compared with the side chain (in α-Asp). While the NMR data are consistent with this explanation, it is conceivable that similar spectral changes might be expected to occur if the observed isomers were due to racemization of Asp9 (i.e. glycopeptides which have D- or L-Asp9). However, this explanation can be eliminated on chemical, analytical and chromatographical grounds. First, although

many biology-related papers, including those studying the proteinaceous aggregates of Alzheimer's disease, consider the succinimide derivative as the transitional product for racemization of aspartic acid residues with a half-time of the reaction stated to be less than a day [40,41], such racemization would require proton loss from the α-carbon of the succinimide, an event largely ignored in the current peptide synthesis literature [32,33]. What was actually measured in one of the basic reference biology papers, when the spontaneous degradation of proteins was modeled, was L-isoaspartic acid bond formation rather than racemization leading to D-aspartic acid containing peptides [42]. Second, the Edman-degradation will not stop at D-aspartic acid residues, but we clearly detected a termination of the sequencing of the earlier eluting glycopeptide at Asp9. Third, the over 1 min retention time difference between the two τR4 glycopeptides on the RP-HPLC chromatogram is unlikely to occur if L-Asp9 was replaced with D-Asp9. Indeed, we did not find any alteration in the HPLC retention time when in an all L-amino acid containing 20-mer peptide both terminal L-amino acids were replaced with their D-enantiomers.

The possibility of the two glycopeptides involving *cis*/*trans* isomerization about the Val-Pro bond was eliminated based on the 2D NMR spectra. In any case the Pro residue is quite distant from the glycosylation site and it is unlikely that glycosylation might induce a differential effect at this distant residue. It is also unlikely that *cis*/*trans* isomers would have displayed the stability observed after HPLC separation, i.e. re-equilibration to a mixture of isomers of each of the purified peaks would have been expected.

The β-glycopeptide eluted at a lower acetonitrile concentration from the RP-HPLC column than the α-isomer, and this is in accordance with the retention behavior of a number of other α-, β-peptide pairs we made earlier [43]. This is also in accordance with the general observation that peptides primarily bind to the reversed-phase column with their side-chain functions (that are characterized with well-defined hydrophobicity parameters) rather than by binding with their backbone [44]. In this regard, it was interesting to note that the isoaspartic-acid bond-containing glycopeptide eluted later than the 'normal' glycopeptide before NaOH treatment, when the sugar-hydroxyl groups were still acetylated. Removal of the acetyl groups resulted in an expected degree of retention time decrease for the α-glycopeptide (2.9 min), but an unusually high retention time decrease of the β-glycopeptide (4.9 min). This indicates that secondary mechanism(s) played a role in the strong column binding of the acetylated and isomerized glycopeptide. Stronger than calculated binding to the RP-HPLC columns [45] can be observed for peptides in which conformational effects display long, conjugated hydrophobic surfaces at one side of the molecules, be those α-helices [46] or β-pleated sheets [47]. To investigate whether the acetylated β-glycopeptide had a similar conjugated hydrophobic surface compared to the acetylated α-glycopeptide, we modeled these molecules with the algorithm described earlier in this discussion. All other protecting groups, not present at the point when the peptides were applied to the RP-HPLC column, were removed before the modeling. As before, the four randomly selected structures from the high temperature trajectory of the simulation within each glycopeptide were remarkably similar. The structures of the α-glycopeptide, however, were markedly different from those of the β-isomer. Plate 1 shows representative structures for the two peptides. The hydrophobic side chains (as well as the carbohydrate with the protecting hydrophobic acetyl groups) are depicted in red. As the bottom model demonstrates, the 'normal' glycopeptide lacks any extended hydrophobic surface. In contrast, the low energy conformer of the isomerized glycopeptide (upper model), displays a long, conjugated hydrophobic surface that runs through one side of the molecule (the bottom side of the model in the presented layout). The conformational orientation explains the higher than expected retention time of the acetylated β-glycopeptide. This conformational orientation was absent in any model of the final (deacetylated) glycopeptides, regardless of whether they corresponded to the α- or the β-glycopeptide, fully supporting the expected order of RP-HPLC elution after deacetylation.

The observed aspartic acid-bond isomerization during the synthesis of a glycopeptide when the non-glycosylated analog was not isomerized is interesting in its own right. However, the high degree of β-peptide formation of our particular glycosylated τ fourth repeat peptide has significance beyond the synthetic chemistry. An *N*-glycosylated version of the τ protein is present only in the PHFs of Alzheimer's disease, but not in normal cerebral τ [19]. Not all potential *N*-glycosylation sites are indeed utilized in natural proteins [36], and sugar occupation in otherwise possibly unutilized glycosylation sites *in vivo* may be a pathobiochemical event, as we have previously demonstrated with the

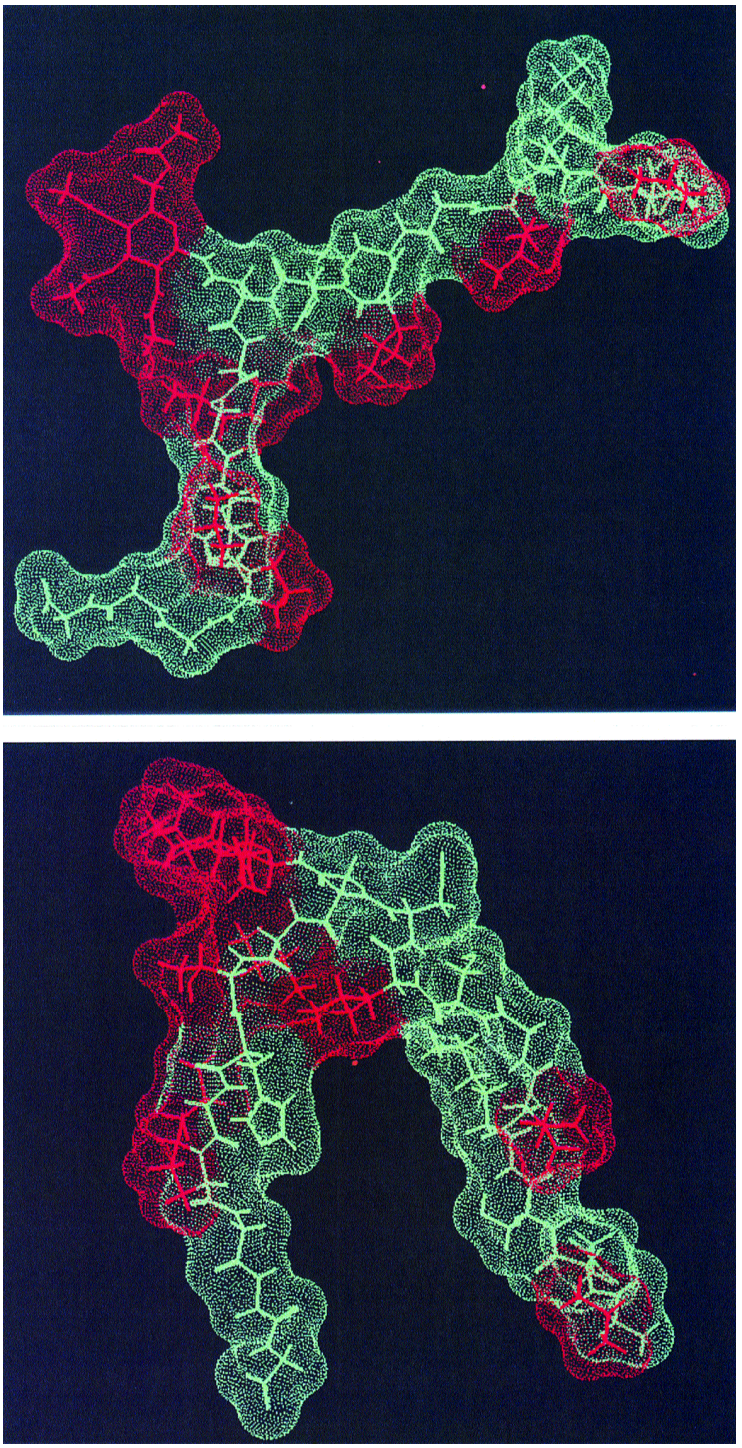

Plate 1 Typical low energy conformers of sugar-protected glycopeptides τR4 Ac_3 GlcNAc carrying either α-(bottom model) or β-(top model)Asp9-Asn10 bonds. The hydrophobic surfaces of the side-chains are shown in red. While these hydrophobic surfaces are scattered around for the 'normal' peptide, they are aligned at one side of the molecule for the isomerized peptide, generating an extended surface that can strongly bind to the reversed-phase packing material.

golli-myelin basic protein, involved in the development of multiple sclerosis [48]. In this regard, it seems significant that the sugar occupancy is normally less extensive at the *C*-terminal regions of the proteins [36], where the potential *N*-glycosylation sites of τ are located. Glycosylated τR4 fails to bind to the corresponding β-tubulin sequence [21], and this may explain the lack of functional τ when it is glycosylated, but this itself does not explain why τ is aggregated in PHF. After all, *N*-glycosylation is expected to break ordered structures such as α-helices [6] and presumably β-pleated sheets, although a local straightening of the peptide backbone was most recently found after O-glycosylation of a natural antibacterial glycopeptide [49]. However, when an excessive glycosylation of τ *in vivo* is accompanied by nearby aspartic acid-bond isomerization the deposition process can proceed. Although the reaction conditions during solid-phase peptide synthesis can hardly model the environment of *in vivo* transformation of proteins, the thermodynamically favored end-products can be very similar in nature. Conjugative degradation of aspartyl peptides is proposed to be an alternative route to irreversible denaturation of proteins regardless of the reaction conditions [50]. Indeed, isoaspartic-acid bond-containing variants of the Aβ peptide, the main constituent of the senile plaques of Alzheimer's disease are detected in the parenchyma and leptomeningeal microvasculature of the brains of affected patients [41]. The β-aspartate containing Aβ fragments exhibit an increased resistance to proteolytic cleavage [51] which may explain why Aβ is retained in the brains. β-Aspartates were also detected in the neurofibrillary tangles of Alzheimer's disease [40], and although the exact composition of the NFT is still unknown, the major proteinaceous constituents of it are known to be τ proteins [17], so the β-aspartate formation in NFT likely involves τ. While the current report was assembled, Asn381 and Asp387 of τ were reported to undergo a deamination process and isoaspartic acid-bond formation [52]. The authors claim that this transformation is responsible for the dimerization and trimerization of τ and thus for PHF formation [52]. In turn, while glycosylation nearby appears to be a readily detectable marker of the pathogenic transformation of τ *in vivo*, the real structural and stability modifications may be provided by the isoaspartic acid-bond formation that is promoted by the sugar addition. This hypothesis is currently being tested in our laboratory using a combination of immunological and peptide stability techniques.

Acknowledgements

The authors wish to thank Drs John Wade and Ronen Marmorstein for helpful suggestions. The second synthesis of peptide τR4 was performed by Carsten Boenke at BMFZ. This work was supported by NIH grant GM 45011 (to L.O.). D.J. Craik is an Australian Research Council Senior Fellow.

REFERENCES

1. Kihlberg J, Eloffson M, Salvador LA. Direct synthesis of glycosylated amino acids from carbohydrate peracetates and Fmoc amino acids: solid-phase synthesis of biomedicinally interesting glycopeptides. In *Methods in Enzymology*, *Solid-Phase Peptide Synthesis*, vol. 289, Fields GB (ed.). Academic Press: San Diego, 1997; 221–245.
2. Perich JW. Synthesis of phosphopeptides using modern chemical approaches. In *Methods in Enzymology*, *Solid-Phase Peptide Synthesis*, vol. 289, Fields GB (ed.). Academic Press: San Diego, 1997; 245–266.
3. Meldal M, St. Hilaire PM. Synthesis methods of Glycopeptide assembly, and biological analysis of glycopeptide products. *Curr. Opin. Chem. Biol.* 1997; **1**: 552–563.
4. Haurum JS, Arsequell G, Lellouch AC, Wong SYC, Dwek RA, McMichael AJ, Elliott T. Recognition of carbohydrate by major histocompatibility complex class I-restricted, glycopeptide-specific cytotoxic T lymphocytes. *J. Exp. Med.* 1994; **180**: 739–744.
5. Hoffmann R, Lee VM-Y, Leight S, Varga I, Otvos Jr L. Unique Alzheimer's disease paired helical filament specific antibodies involve double phosphorylation at specific sites. *Biochemistry* 1997; **36**: 8114–8124.
6. Otvos Jr L, Thurin J, Kollat E, Urge L, Mantsch HH, Hollosi MM. Glycosylation of synthetic peptides breaks helices; phosphorylation results in distorted structure. *Int. J. Pept. Protein Res.* 1991; **38**: 476–482.
7. Otvos Jr L,Cappelletto B, Varga I, Xiang ZQ, Kaiser K, Stephens LDJ, Ertl HCJ. Comparison of the effects of post-translational side-chain modifications on the serum stability, T helper cell stimulatory activity and conformation of synthetic peptides. *Biochim. Biophys. Acta* 1996; **1267**: 55–64.
8. Polt R, Porreca F, Szabo LZ, Bilsky EJ, Davis P, Abbruscato TJ, Davis TP, Horvath R, Yamamura HI, Hruby VJ. Glycopeptide enkephalin analogues produce analgesia in mice: evidence for penetration of the blood–brain barrier. *Proc. Natl. Acad. Sci. USA* 1994; **91**: 7114–7118.
9. Kitas EA, Johns RB, May CN, Tregear GW, Wade JD. Chemical synthesis of an *O*-phosphorylated tyrosine analogue of human angiotensin II, [Tyr(P)4] angiotensin II, and its vasoconstrictor effect in intact sheep. *Pept. Res.* 1993; **3**: 205–210.

10. Garg HG, von dem Bruch K, Kunz H. Developments in the synthesis of glycopeptides containing glycosyl L-asparagine, L-serine, and L-threonine. *Adv. Carbohydr. Chem. Biochem.* 1994; **50**: 277–310.
11. Arsequell, G, Valencia G. *O*-glycosyl α-amino acids as building blocks for glycopeptide synthesis. *Tetrahedron: Asymmetry* 1997; **8**: 2839–2876.
12. Taylor CM. Glycopeptides and glycoproteins: focus on the glycosidic linkage. *Tetrahedron* 1998; **54**: 11317–11362.
13. Otvos Jr L, Wroblewski K, Kollat E, Perczel A, Hollosi M, Fasman GD, Ertl HCJ, Thurin J. Coupling strategies in solid-phase synthesis of glycopeptides. *Pept. Res.* 1989; **2**: 362–366.
14. Otvos Jr L, Urge L, Hollosi M, Wroblewski K, Graczyk G, Fasman GD, Thurin J. Automated solid-phase synthesis of glycopeptides. Incorporation of unprotected mono- and disaccharide units of N-glycoprotein antennae into T cell epitopic peptides. *Tetrahedron Lett.* 1990; **31**: 5889–5892.
15. Goedert M, Spillantini MG, Jakes R, Rutherford D, Crowther RA. Multiple isoforms of human microtubule-associated protein Tau: sequences and localization in neurofibrillary tangles of Alzheimer's disease. *Neuron* 1989; **3**: 519–526.
16. Kirschner DA, Abraham C, Selkoe DJ. X-ray diffraction from intraneuronal paired helical filaments and extraneuronal amyloid fibers in Alzheimer's disease indicates cross-β conformation. *Proc. Natl. Acad. Sci. USA* 1986; **84**: 6953–6957.
17. Lee VM-Y, Balin BJ, Otvos Jr L, Trojanowski JQ. A68: a major subunit of paired helical filaments and derivatized forms of normal Tau. *Science* 1991; **251**: 675–678.
18. Wille H, Drewes G, Biernat J, Mandelkow E-M, Mandelkow E. Alzheimer-like paired helical filaments and antiparallel dimers formed from microtubule-associated protein Tau *in vitro*. *J. Cell Biol.* 1992; **118**: 573–584.
19. Wang, J-Z, Grundke-Iqbal I, Iqbal K. Glycosylation of microtubule-associated protein Tau: an abnormal posttranslational modification in Alzheimer's disease. *Nature Med.* 1996; **2**: 871–875.
20. Butner KA, Kirschner MW. Tau protein binds to microtubules through a flexible array of distributed weak sites. *J. Cell Biol.* 1991; **115**: 717–730.
21. Otvos Jr L, Pease A-M, Wade JD, Hoffmann R. Glycosylation of the fourth repeat unit of human τ protein abolishes binding to the C-terminal acidic τ-binding segment of β-tubulin. *Protein Peptide Lett.* 1998; **5**: 207–213.
22. Fields GB, Noble RL. Solid-phase peptide synthesis using 9-fluorenylmethoxycarbonyl amino acids. *Int. J. Pept. Protein Res.* 1990; **35**: 161–214.
23. Kaiser E, Colescott RL, Bossinger CD, Cook PI. Color test for detection of free terminal amino groups in the solid-phase synthesis of peptides. *Anal. Biochem.* 1970; **34**: 595–598.
24. Bulet P, Urge L, Ohresser S, Hetru C, Otvos Jr L. Enlarged scale chemical synthesis and range of activity of Drosocin, an *O*-glycosylated antibacterial peptide from Drosophila. *Eur. J. Biochem.* 1996; **238**: 64–69.
25. Fasman GD. A critique of the utility of the prediction of protein secondary structure. *J. Biosci.* 1985; **8**: 15–23.
26. Brooks BR, Bruccoleri RE, Olafson BD, States DJ, Swaminathan S, Karplus M. CHARMm: a program for macromolecular energy minimization and dynamics calculations. *J. Comput. Chem.* 1983; **4**: 187–217.
27. Marion D, Wüthrich K. Applications of phase sensitive two-dimensional correlated spectroscopy (COSY) for measurements of ^1H–^1H spin–spin coupling constants in proteins. *Biochem. Biophys. Res. Comm.* 1983; **113**: 967–974.
28. Bax A, Davis DG. MLEV-17 based two-dimensional homonuclear magnetization transfer spectroscopy. *J. Mag. Res.* 1985; **65**: 355–360.
29. Otvos Jr L, Urge L, Szendrei GI, Cappelletto B, Varga I, Prammer K, Ertl HCJ. Exploring the diversity of mono- and oligosaccharide structures in the synthesis, conformational analysis and biomedical application of glycopeptides. In *Solid-Phase Synthesis and Combinatorial Libraries*, Epton R (ed.). Mayflower Scientific: Birmigham, 1996; 269–276.
30. Otvos Jr L, Krivulka GR, Urge L, Szendrei GI, Nagy L, Xiang ZQ, Ertl HCJ. Comparison of the effects of amino acid substitutions and β-N- vs. α-O-glycosylation on the T-cell stimulatory activity and conformation of an epitope on the rabies virus glycoprotein. *Biochim. Biophys. Acta* 1995; **1267**: 55–64.
31. Hoffmann R, Bulet P, Urge L, Otvos Jr L. Range of activity and metabolic stability of synthetic antibacterial glycopeptides from insects. *Biochim. Biophys. Acta* 1999; **1426**: 459–467.
32. Barany G, Merrifield RB. Solid-phase peptide synthesis. In *The Peptides*, vol. 2, Gross E, Meienhofer J (eds). Academic Press: New York, 1979; 1–284.
33. Bodanszky M, Martinez J. Side reactions in peptide synthesis. In *The Peptides*, vol. 5, Gross E, Meienhofer J (eds). Academic Press: New York, 1983; 111–216.
34. Lauer JL, Fields CG, Fields GB. Sequence dependence of aspartimide formation during 9-fluorenylmethoxycarbonyl solid-phase peptide synthesis. *Lett. Pept. Sci.* 1994; **1**: 197–205.
35. Dolling R, Beyermann M, Haenel J, Kernchen F, Krause E, Franke P, Brudel M, Bienert M. Piperidine-mediated side reactions in Fmoc-strategy. In *Solid-Phase Synthesis and Combinatorial Libraries*, Epton R (ed). Mayflower Worldwide: Birmingham, 1994; 489–492.
36. Gavel Y, von Heijne G. Sequence differences between glycosylated and non-glycosylated Asn-X-Thr/Ser acceptor sites: implications in protein engineering. *Prot. Eng.* 1990; **3**: 433–442.
37. Robinson AB, Robinson LR. Distribution of glutamine and asparagine residues and their near neighbors in

peptides and proteins. *Proc. Natl. Acad. Sci. USA* 1991; **88**: 8880–8884.
38. Urge L, Kollat E, Hollosi M, Laczko I, Wroblewski K, Thurin J, Otvos Jr L. Solid-phase synthesis of glycopeptides: synthesis of *N*-α-fluorenylmethoxycarbonyl L-asparagine *N*-β-glycosides. *Tetrahedron Lett*. 1991; **32**: 3445–3448.
39. Angell YM, Garcia-Echeverria C, Rich DH. Comparative studies of the coupling of N-methylated, sterically hindered amino acids during solid-phase peptide synthesis. *Tetrahedron Lett*. 1994; **35**: 5891–5894.
40. Payan IL, Chou S-J, Fisher GH, Man EH, Emory C, Frey II WH. Altered aspartate in Alzheimer neurofibrillary tangles. *Neurochem. Res*. 1992; **17**: 187–191.
41. Roher AE, Lowenson JD, Clarke S, Wolkow C, Wang R, Cotter RJ, Reardon IM, Zurcher-Neely HA, Heinrikson RL, Ball M, Greenberg BD. Structural alterations in the peptide backbone of β-amyloid core protein may account for its deposition and stability in Alzheimer's disease. *J. Biol. Chem*. 1993; **268**: 3072–3083.
42. Stephenson RC, Clarke S. Succinimide formation from aspartyl and asparaginyl peptides as a model for the spontaneous degradation of proteins. *J. Biol. Chem*. 1989; **264**: 6164–6170.
43. Szendrei GI, Fabian H, Mantsch HH, Lovas S, Nyeki O, Schon I, Otvos Jr L. Aspartate-bond isomerization affects the major conformations of synthetic peptides. *Eur. J. Biochem*. 1994; **226**: 917–924.
44. Meek JJ. Prediction of peptide retention times in high-pressure liquid chromatography on the basis of amino acid composition. *Proc. Natl. Acad. Sci. USA* 1988; **77**: 1632–1636.
45. Browne CA, Bennett HP, Solomon S. The isolation of peptides by high-performance liquid chromatography using predicted elution positions. *Anal. Biochem*. 1982; **124**: 201–208.
46. Buttner K, Pinilla C, Appel JR, Houghten RA. Anomalous reversed-phase high performance liquid chromatographic behavior of synthetic peptides related to antigenic helper T cell lines. *J. Chromatogr*. 1992; **625**: 191–198.
47. Hearn MTW, Aguilar MI. High performance liquid chromatography of amino acids, peptides and proteins LXIX. Evaluation of retention and bandwidth relationships of myosin-related peptides separated by gradient elution reverse-phase high performance liquid chromatography. *J. Chromatogr*. 1987; **392**: 33–49.
48. Clark L, Otvos Jr L, Stein P, Zhang X-M, Skorupa AF, Lesh GE, McMorris FA, Heber-Katz E. Golli-induced paralysis: a study in anergy and disease. *J. Immunol*. 1999; **162**: 4300–4310.
49. McManus A, Otvos Jr L, Hoffmann R, Craik DJ. Conformational studies by NMR of the anti-microbial peptide, Drosocin and its non-glycosylated derivative: effects of glycosylation on solution conformation. *Biochemistry* 1999; **38**: 705–714.
50. Schon I, Nyeki O. Unprecedented transformation of aspartyl peptides by conjugative degradation. *J. Chem. Soc. Chem. Commun*. 1994; 393–394.
51. Szendrei GI, Prammer KV, VaskoM, Lee VM-Y, Otvos Jr L. The effects of aspartic acid bond isomerization on *in vitro* properties of the amyloid β-peptide as modeled with N-terminal decapeptide fragments. *Int. J. Pept. Protein Res*. 1996; **47**: 289–296.
52. Watanabe A, Takio K, Ihara Y. Deamination and isoaspartate formation in smeared tau in paired helical filaments: unusual properties of the microtubule-binding domain of tau. *J. Biol. Chem*. 1999; **274**: 7368–7378.

